Sensors and Actuators B 224 (2016) 592–599

Contents lists available at ScienceDirect

Sensors and Actuators B: Chemical

journal homepage: www.elsevier.com/locate/snb

Novel colorimetric and fluorescent off–on enantiomers with high selectivity for Fe^{3+} imaging in living cells

Chunhua Fan [a], Ximing Huang [a], Liheng Han [b], Zhengliang Lu [a,*], Zhuo Wang [c,*], Yuanping Yi [b,*]

[a] School of Chemistry and Chemical Engineering, University of Jinan, Jinan 250022, China
[b] Beijing National Laboratory for Molecular Sciences, CAS Key Laboratory of Organic Solids, Institute of Chemistry, Chinese Academy of Sciences, Beijing 100190, China
[c] Faculty of Science, Beijing University of Chemical Technology, Beijing 100029, China

ARTICLE INFO

Article history:
Received 31 July 2015
Received in revised form 26 October 2015
Accepted 28 October 2015
Available online 31 October 2015

Keywords:
Chirality
Fluorescent chemosensor
Iron
Living cell

ABSTRACT

Two novel colorimetric and fluorescent off–on enantiomers (*R*/*S*-**RBOL**) were developed to detect Fe^{3+} in aqueous and biological samples through probing the integrated changes in fluorescence, circular dichroism (CD) and circularly polarized luminescence (CPL). The fluorescence intensity of *R*/*S*-**RBOL** is linearly proportional to the Fe^{3+} concentration in the range of 0–20 equiv., bringing out a detection limit of 1.83×10^{-7} M. The Job's plot indicates a 1:1 binding stoichiometry of **RBOL**:Fe^{3+}, which is further confirmed by ESI-MS analysis. Moreover, the **RBOL**s exhibit a dual-readout response in colour and fluorescence, rendering them suitable to sense Fe^{3+} in living cells with low cytotoxicity. In order to shed some light on the detection mechanism, the coordination between *R*/*S*-**RBOL** and Fe^{3+} is unravelled by DFT calculations. From the free **RBOL** to the **RBOL**–Fe^{3+} complex, the spiro-lactam ring is opened to interact with Fe^{3+} via the lactam N and O, imine N and hydroxyl O atoms in the form of a ferric six-coordinate structure.

1. Introduction

The developments of selective chemosensors for detection of transition- and heavy-metal ions are of extensively significant interest in recent years, due to their real-time monitoring capability for metal ions in many biological processes at the cellular level [1–6]. Till date, selective fluorescent chemosensors for Fe^{3+} have been rarely reported compared to the ones for detection of the hazardous metals, such as Hg^{2+}, Pb^{2+}, Cd^{2+} [7–10], and it is probably owing to the interference of other cations, such as Cu^{2+} and Cr^{3+} [11–13]. However, the easy and accurate detection of Fe^{3+}, one of the most essential trace metals within human and animal bodies, has attracted more and more attention because of the biological significance of Fe^{3+} in protein synthesis, enzymatic catalysis, oxygen transportation and cellular metabolism [14–18]. Low Fe^{3+} concentration in biosystems could cause a variety of disorders, such as iron deficiency anaemia, neurodegenerative diseases (e.g. Alzheimer's, Huntington's, and Parkinson's diseases), while overload of iron might oxidize and finally damage lipids, proteins and other cellular components by reactive oxygen species (ROS) rising from the Fenton reaction [19–23]. Currently, many chemosensors reported have been developed based on the fluorescence turn-off [24–27] or turn-on [28–33] mechanism for highly selective detection of Fe^{3+} over other interfering heavy metal ions.

In contrast, it is rarely reported to detect metal ions with chiral chemosensors, which can be constructed based on the combination of a chiral moiety and a fluorophore as a signalling site [34,35]. Most importantly, since those chiral sensors are possible to show circular dichroism (CD) and circularly polarized luminescence (CPL) signals, they have been used to design CPL organic molecules to elucidate chiral structures in the excited state [36] and have potential applications in enantioselective CPL chemosensors [37], biological probes [38–41], 3D optical displays [42] or light-emission systems for asymmetric photosynthesis [43–45]. Currently, many CD and CPL molecules are designed to contain a intrinsic fluorophore, such as BODIPY [46–48]. It is well known that the structural transformations between the spirocyclic moiety and open form of rhodamine are sensitive and susceptible to the stimulation of guests; the open form gives a red colour and has a strongly fluorescent light-up effect. The colour and fluorescence dual responses can sensitively indicate the level of guest metals in living cells, such as Pd^{2+}, Cu^{2+},

* Corresponding author.
E-mail addresses: zhengliang.lu@yahoo.com (Z. Lu), wangzhuo77@mail.bust.edu.cn (Z. Wang), ypyi@iccas.ac.cn (Y. Yi).

http://dx.doi.org/10.1016/j.snb.2015.10.104
0925-4005/

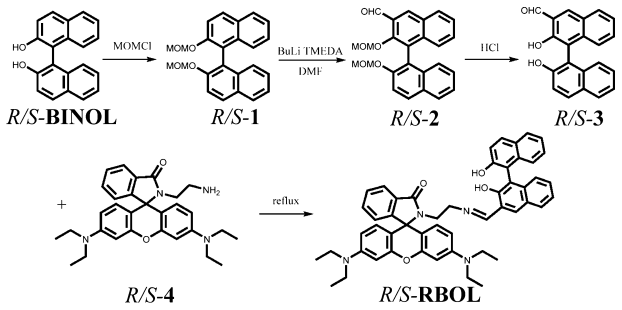

Scheme 1. Synthesis of *R*/*S*-**RBOL**.

Fe^{3+} [49–51]. So we speculated that the combination of rhomadine and chiral moiety might lead to a kind of chiral chemosensors that are able to sense metal ions in living cells and to produce CD and CPL signals simutaneously based on the binding of metal ions.

According to this speculation, we synthesized two novel cell-permeable colorimetric and fluorescent off–on enantiomers (*R*/*S*-**RBOL**) based on the rhodamine derivatives to selectively and sensitively detect Fe^{3+}. For these chiral fluorescent organic molecules, the *R*/*S*-1,1′-binaphthol moiety is found to act as an excellent binding and chiral barrier site for producing CD and CPL signals.

2. Materials and methods

2.1. Instruments and chemicals

All the starting chemicals were of AR grade and used as received unless otherwise stated. Water used in experiments was purified by a Milli-Q system (Millipore, USA). Solutions of K^+, Na^+, Li^+, Mn^{2+}, Ni^{2+}, Cd^{2+},Pb^{2+}, Fe^{2+}, Al^{3+} and Cr^{3+} were prepared from their chloride or sulfate salts; solutions of Ba^{2+}, Fe^{3+}, Ag^+, Cu^{2+}, Zn^{2+} and Hg^{2+} were prepared from their nitrate salts. 2-(2-aminoethyl)-3′,6′-bis(diethylamino)spiro[isoindoline-1,9′-xanthen]-3-one (**4**) and chiral 1,1′-binaphthalene-3-carboxaldehydes (*R*/*S*-**3**) as well as **1**, **2** and **3** were synthesized following revised procedures [52–55]. ^1H NMR and ^{13}C NMR spectra were collected on a Bruker DRX-400 spectrometer using TMS as an internal standard. MS spectra were obtained on a PE Sciex API 3000 mass spectrometer or a Bruker autoflex III MALDI-TOF mass spectrometer. Elemental analyses (C, H, N) were performed on a Perkin-Elmer 240 analyzer. The pH was measured with a Metrohm 808 Titrando pH meter. All fluorescence measurements were recorded using a F380 fluorescence spectrometer. UV–vis absorption spectra were carried out with a Shimadzu UV-2450 spectrophotometer. Circular dichroism (CD) and circularly polarized luminescence (CPL) spectra were performed on a JASCO J-810 and JASCO CPL-200 spectrofluoropolarimeter, respectively. Confocal fluorescence imaging studies were performed with a Zeiss laser scanning microscope 710 (Carl Zeiss).

2.2. Synthesis of R/S-*RBOL*

The solution containing **4** (0.2824 g, 0.6 mmol) and enantiopure *R*-**3** or *S*-**3** (0.1574 g, 0.5 mmol) in ethanol (20 mL) was refluxed for 6 h. After cooling, the precipitate was filtered and washed with ethanol and finally gave *R*/*S*-**RBOL** as a light yellow solid. *R*-**RBOL**: (0.25 g, 72.0%). ^1H NMR (400 MHz, $CDCl_3$) δ ppm: 13.47 (s, 1H), 8.46 (s, 1H), 7.82–7.91 (m, 5H), 7.43 (dd, J = 5.75, 2.99 Hz, 2H), 7.27–7.36 (m, 4H), 7.19 (td, J = 8.28, 1.26 Hz, 1H), 7.14 (d, J = 7.53, 1H), 7.07 (m, 2H), 6.42 (d, J = 2.56 Hz, 1H), 6.40 (d, J = 2.54 Hz, 1H), 6.33 (dd, J = 7.08, 2.48 Hz, 2H), 6.23 (dt, J = 8.92, 2.20 Hz, 2H), 5.15 (s, 1H), 3.35–3.46 (m, 4H), 3.27 (ddd, J = 9.14, 7.12, 2.37 Hz, 8H), 1.13 (td, J = 6.86, 1.08 Hz, 12H). ^{13}C NMR (100 MHz, $CDCl_3$) δ ppm:

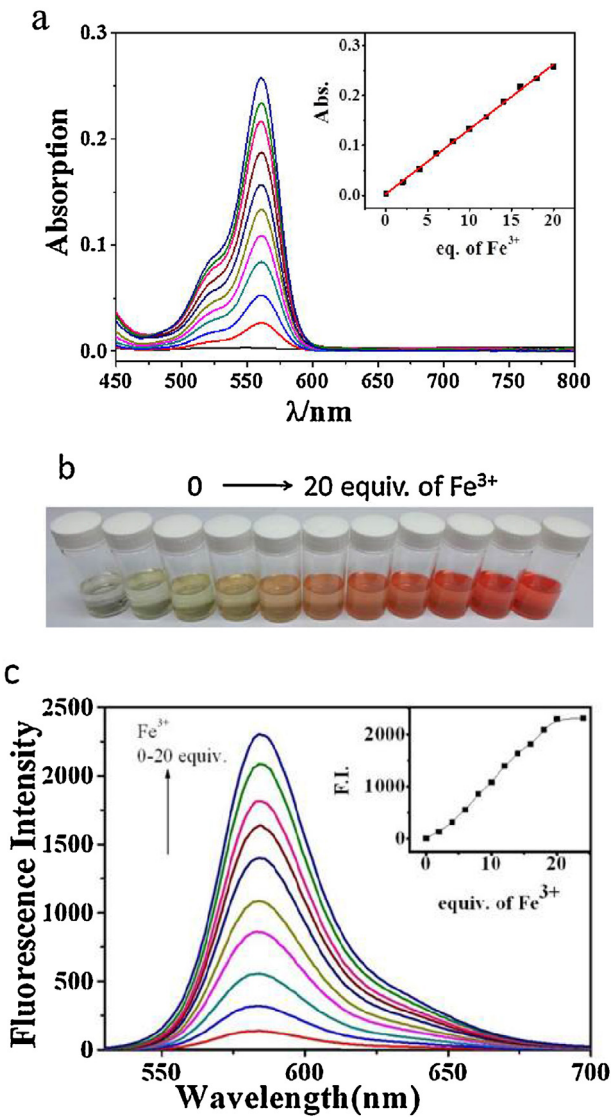

Fig. 1. (a) UV–vis spectra of *R*-**RBOL** (50 μM) in THF/H_2O (v/v, 3/7, HEPES = 10 mM/L) at different concentrations of Fe^{3+} ions (0, 2, 4, 6, 8, 10, 12, 14, 16, 18 and 20 equiv.). (b) Colour changes of *R*-**RBOL** in the visible region upon addition of different Fe^{3+} concentration (0–20 equiv.). (c) Fluorescence emission spectra of *R*-**RBOL** (50 μM) with the excitation at 510 nm, upon the titration of Fe^{3+} (0–20 equiv.) in a THF/H_2O (v/v, 3/7, HEPES, 10 mM, pH 7.0) solution. Inset: the linear response curve of emission intensity of *R*-**RBOL** at 585 nm depending on Fe^{3+} concentration.

168.3, 165.8, 155.7, 153.6, 151.6, 148.9, 135.3, 134.1, 130.9, 129.3, 128.6, 127.5, 126.5, 124.7, 123.8, 122.8, 120.9, 117.8, 114.6, 113.7, 108.1, 105.1, 97.9, 65.0, 57.1, 44.3, 40.8, 12.6. MS calculated for $C_{51}H_{48}N_4O_4$ $[M+H]^+$ 781.37, found 781.5. *S*-**RBOL**: (0.22 g, 63.4%). Anal. Calcd. for $C_{51}H_{48}N_4O_4$: C, 78.44; H, 6.20; N, 7.17. Found C, 78.39; H, 6.25; N, 7.14.

2.3. Calculations

The molecular geometries for **RBOL** and **RBOL**–$FeCl_2^+$ were optimized by density functional theory (DFT). Based on the optimized geometries, the excited-state properties and UV–vis spectra were computed by time-dependent DFT (TDDFT) and the polarizable continuum model (PCM) was used to consider the solvent effects. All these calculations were carried out with the Becke-3–Lee–Yang–Parr (B3LYP) exchange functional and a mixed